

Phase transition in a four-dimensional fermion model

Syôzi Kawati and Hidenori Miyata

Department of Physics, Kwansei Gakuin University, Nishinomiya 662, Japan

(Received 6 January 1981)

We study the four-dimensional self-coupled massless fermion model with a dynamical breakdown of chiral symmetry through an emergence of collective excitations and discuss a phase transition under the influence of both temperature T and fermion-number density n . We give the self-consistency equation which determines an amount of dynamically generated fermion mass as a function of T and n . Using the numerical solutions of the self-consistency equation, we derive the effective potential of the collective excitations. We show that the model has a second-order phase transition at a critical temperature and also at a critical density and that the dynamical symmetry violation vanishes above these critical values. We also draw the phase diagram in the T - n plane for several values of the generated fermion mass.

I. INTRODUCTION

The study of symmetry behavior dependent on temperature and density in elementary particle systems has become an interesting area in physics, e.g., the hot early universe, the pion-condensed state of neutron stars, and the highly excited nuclear matter in a central collision of nuclei. Since Kirzhnits and Linde¹ first suggested that by the analogy of the Meissner effect, spontaneous symmetry breakdown in relativistic field theory will be restored above a critical temperature, many authors have examined various field theories exhibiting spontaneous symmetry violation at an increase of temperature and density. They have shown that symmetry violation at zero or at low temperature will disappear as temperature increases, i.e., at a critical temperature the phase transition from a symmetry-broken state to a normal one takes place.²⁻¹² A similar phenomenon has also been investigated in high-density matter.¹³⁻¹⁷ There exists a critical density at which the phase transition occurs.

Besides models of spontaneous symmetry breakdown with the presence of a tachyon field in the original Lagrangian, some dynamical-symmetry-broken models are known and some of them show a phase transition at a critical temperature and a critical density. Recently, Gross and Neveu¹⁸ have verified that the N -component, massless Thirring model in $1+1$ dimension shows dynamical violation of chiral symmetry through generating fermion mass at zero temperature and in the absence of fermion density. Subsequent to their work, it has been shown that this dynamical symmetry violation in $1+1$ space-time vanishes above the critical temperature and above the critical density, and then the chiral symmetry can be restored.¹⁹⁻²²

In this paper we investigate a four-dimensional

fermion model with a dynamical symmetry breakdown, and discuss the behavior of the phase transition under the influence of both temperature and fermion density. Our model is defined by the Lagrangian

$$\mathcal{L} = \bar{\psi} i \not{\partial} \psi + \frac{1}{2} \kappa^2 (\bar{\psi} \psi)^2, \quad (1.1)$$

where ψ is a Dirac spinor field in $(3+1)$ -dimensional space-time and κ denotes the four-fermion coupling with a dimension of $(\text{mass})^{-2}$. It is obvious that this Lagrangian has a symmetry under the chiral transformation $\psi \rightarrow \gamma_5 \psi$. The advantage for us to adopt this model is due to the fact that it has dynamical symmetry breaking through the emergence of collective excitations.²³⁻²⁶ It looks unrenormalizable in the perturbation expansion with respect to the four-fermion coupling κ , but if the theory could develop a bound state or a collective mode (the Cooper pair in the context of the theory of superconductivity), it has a renormalizable perturbation series with respect to the coupling constant between the fermion and collective mode. And this series, resummed by the Hartree approximation or the mean-field expansion, is equivalent in structure to the perturbation series for the renormalizable Yukawa-type theory.²⁷⁻³¹ In the present work, we do not refer to the mechanism by which the theory develops the bound states, and it is assumed that there exists a bound state and the violation of chiral symmetry is caused by a nonvanishing vacuum expectation value of generated bound states. Our interest is in the effect of temperature and fermion density in the four-dimensional theory with dynamical symmetry breakdown.

In the next section we consider the broken-symmetry model of $3+1$ space-time without influence of both temperature and number density, which is governed by an ordinary field theory within the Hartree approximation. As is usually done for

the discussion of symmetry breakdown, we calculate the effective potential for the uniform collective mode. Our model contains ultraviolet divergences that come from fermion one-loop diagrams, and they are all handled by the dimensional regularization method in $4 - \epsilon$ space-time dimensions. The ϵ^{-1} -dependent terms are absorbed in the theory with renormalization prescriptions. But, as will be seen later, the renormalized coupling constant between the fermion and collective modes is not dependent on the bare one; then it becomes an unfixed number in the limit $\epsilon \rightarrow 0$. So we must keep ϵ nonzero and small. This is characteristic of the type of four-fermion theory within the Hartree approximation that has already been commented on in our recent work.²⁷ It means that although ϵ does not appear in the final expression of the effective potential, the model contains ϵ implicitly in the "renormalized coupling constant", so our treatment of the model is somewhat phenomenological.³²

In Sec. III, we develop the general formulation for the model defined in Sec. II under the influence of both temperature and chemical potential, and give the self-consistency equation which determines the amount of dynamically generated fermion mass as a function of temperature and fermion-number density. We also derive the effective potential.

In Sec. IV, we consider the influence only of temperature for the model, based on the formulation in Sec. III in order to clear our central point. The self-consistency equation and the effective potential are calculated analytically in terms of the modified Bessel functions, and the critical temperature T_c , at which the generated fermion mass vanishes and then chiral-symmetry violation is restored, is given by the self-consistency equation. On the other hand, we may define a critical temperature T_c^* at which the propagator of the uniform collective mode diverges. This is the point of inflection of the effective potential in equilibrium. At the later critical point T_c^* , the fermion mass takes a nonzero value and it seems that the broken symmetry is not restored. However, for a small value of the coupling, the nonzero fermion mass could be put to zero in a practical manner, and we can identify that two points T_c and T_c^* coincide in practice; then the model predicts the second-order phase transition. But in general, near the critical temperature, the approximation tends to break down by the appearance of an infrared singularity, which is unavoidable for the dynamical-symmetry-breaking model. These phenomena are discussed in detail. We give a phase diagram and calculate the effective potential and vertices for the collective mode by

numerical analysis.

Section V is devoted to the study of the effect of chemical potential or fermion-number density at absolute zero temperature. Similar phenomena to the temperature phase transition are seen, and also several quantities are plotted graphically.

In Sec. VI, we intend to investigate the model at finite temperature and nonzero fermion-number density, and in this case most quantities cannot be calculated analytically. We analyze the system under both influences by numerical calculation and discuss them. As will be often commented in the later sections, we use the unit $M_0 = 1$ in all numerical calculations and all figures.

II. THE MODEL

We introduce an auxiliary field $\sigma(x)$ and rewrite the Lagrangian (1.1) in terms of the field $\sigma(x)$ equivalently as

$$\mathcal{L}' = \bar{\psi}(i \not{\partial} - g_0 \sigma) \psi - \frac{1}{2} m_0^2 \sigma^2 \quad (2.1)$$

with

$$\kappa^2 = \frac{g_0^2}{m_0^2}, \quad (2.2)$$

where g_0 is a bare dimensionless coupling constant and m_0 represents a parameter with a dimension of mass. It can be easily checked that the Lagrangian (2.1) produces the same generating functional as the Lagrangian (1.1) when an integration over $\sigma(x)$ is performed. Because the original theory Eq. (1.1) contains only one parameter κ , the mass parameter m_0 may be redundant, and so it should be fixed in a self-consistent way, that will be seen later.

Here we assume that the auxiliary field $\sigma(x)$ has a nonvanishing vacuum expectation value,

$$\langle \sigma(x) \rangle = \sigma_0, \quad (2.3)$$

then a fermion mass is generated to an amount of $g_0 \sigma_0$ and the chiral symmetry of the system is violated. So we can see a behavior of the dynamically broken chiral symmetry of the theory through the generated fermion mass.

In the discussion of a symmetry-broken model, the most convenient method is to study the effective potential. In the usual way, we first define the generating functional for the connected Green's function $W[J]$,

$$e^{iW[J]} \equiv \int d\psi d\bar{\psi} d\sigma e^{i \int d^4x (\mathcal{L}' + J\sigma)}, \quad (2.4)$$

where $J(x)$ is an external source coupled to $\sigma(x)$. Then the classical field can be defined as

$$\sigma_c(x) \equiv \frac{\delta W[J]}{\delta J(x)}. \quad (2.5)$$

When the external source $J(x)$ vanishes, the classical field $\sigma_c(x)$ turns into a vacuum expectation value and it is independent of space-time with an assumption of translation invariance. Hereafter we suppress the subscript c of σ_c to simplify the notation. Working with the Legendre transform of $W[J]$, which yields the effective action, we obtain the effective σ potential to the lowest order,

$$V(\sigma) = i \operatorname{tr} \ln(i\not{\partial} - g_0\sigma) + \frac{1}{2}m_0^2\sigma^2. \quad (2.6)$$

The functional logarithm in the above equation consists of an infinite set of one-fermion-loop diagrams with an arbitrary number of zero-four-momentum external σ lines.

Next we fix the redundant parameter m_0 in Eq. (2.6), which looks arbitrary. Because the vacuum expectation value σ_0 is a real stable vacuum of the effective σ potential, it should satisfy the conditions

$$\left. \frac{\partial V}{\partial \sigma} \right|_{\sigma=\sigma_0} = 0 \quad (2.7)$$

and

$$\left. \frac{\partial^2 V}{\partial \sigma^2} \right|_{\sigma=\sigma_0} \geq 0. \quad (2.8)$$

Equation (2.7) with Eq. (2.6) reads

$$m_0^2\sigma_0 = -ig_0 \operatorname{tr} \int \frac{d^4k}{(2\pi)^4} S_F(k), \quad (2.9)$$

where $S_F(k)$ stands for the fermion propagator with the generated mass $M_0 (=g_0\sigma_0)$,

$$S_F(k) = \frac{1}{M_0 - \not{k}}. \quad (2.10)$$

With the dimensional regularization in $4-\epsilon$ space-time and in the limit $\epsilon \rightarrow 0$, we get

$$m_0^2 = -\frac{g_0^2}{4\pi^2} M_0^2 \left(\frac{2}{\epsilon} - \gamma - \ln \frac{M_0^2}{\lambda^2} + 1 \right), \quad (2.11)$$

where γ is Euler's constant and λ is the unit mass,³³ which is introduced so that the physical quantities have correct dimensions in $4-\epsilon$ space-time.

The lowest-order inverse σ propagator is given by

$$\Delta^{-1}(k^2) = m_0^2 - g_0^2 \operatorname{tr} \int \frac{d^4p}{(2\pi)^4} S_F(p+k) S_F(k) \quad (2.12)$$

and the above equation is integrated in $4-\epsilon$ dimensions to be

$$\Delta^{-1}(k^2) = \frac{g_0^2}{4\pi^2} (k^2 - 4M_0^2) \left[\frac{1}{\epsilon} - \frac{\gamma}{2} + 1 - \frac{1}{2} \ln \frac{M_0^2}{\lambda^2} - \frac{1}{2} T \left(-\frac{k^2}{M_0^2} \right) \right], \quad (2.13)$$

where we have used the value of m_0 fixed in Eq. (2.11) and $T(x)$ is defined as follows³⁴:

$$T(x) = \begin{cases} 2 \left(1 + \frac{4}{x} \right)^{1/2} \sinh^{-1} \frac{\sqrt{x}}{2}, & x \geq 0, \\ 2 \left(\frac{4}{|x|} - 1 \right)^{1/2} \sin^{-1} \frac{\sqrt{|x|}}{2}, & -4 \leq x \leq 0, \\ \left(1 - \frac{4}{|x|} \right)^{1/2} \left(2 \cosh^{-1} \frac{\sqrt{|x|}}{2} - i\pi \right), & x \leq -4. \end{cases} \quad (2.14)$$

It is noted by Eq. (2.13) that a bound state appears at the threshold $k^2 = 4M_0^2$ to this order of approximation.

Before the discussion of an effective potential, we give a renormalization prescription. Introducing the lowest-order renormalized mass M_R^2 , a renormalization factor Z , and a renormalized coupling g by³¹

$$\Delta^{-1}(0) = -Z^{-1}M_R^2, \quad (2.15)$$

$$\left. \frac{\partial \Delta^{-1}(k^2)}{\partial k^2} \right|_{k^2=0} = Z^{-1}, \quad (2.16)$$

$$g^2 = Zg_0^2, \quad (2.17)$$

we obtain

$$Z^{-1} = \frac{g_0^2}{4\pi^2} \left(\frac{1}{\epsilon} - \frac{\gamma}{2} - \frac{1}{2} \ln \frac{M_0^2}{\lambda^2} - \frac{1}{3} \right) \quad (2.18)$$

and

$$M_R^2 = 4M_0^2 \left(1 + \frac{g^2}{12\pi^2} \right). \quad (2.19)$$

The renormalized σ propagator Δ_R^{-1} is defined by

$$\Delta_R^{-1} = Z^{-1} \Delta^{-1} \quad (2.20)$$

and turns out to be

$$\Delta_R^{-1}(k^2) = (k^2 - 4M_0^2) \left(1 + \frac{g^2}{3\pi^2} - \frac{g^2}{8\pi^2} T(-k^2/M_0^2) \right). \quad (2.21)$$

The above renormalization prescription results in the definition of a renormalized field σ_R ,

$$\sigma = Z^{1/2} \sigma_R. \quad (2.22)$$

However, Eqs. (2.17) and (2.18) show

$$\frac{1}{g^2} = \frac{1}{4\pi^2} \left(\frac{1}{\epsilon} - \frac{\gamma}{2} - \frac{1}{2} \ln \frac{M_0^2}{\lambda^2} - \frac{1}{3} \right). \quad (2.23)$$

So, as commented in Sec. I, we must keep ϵ a small number not zero, and then choose the renormalized coupling to be a small fixed value of order ϵ .

We go back to the discussion of an effective potential with the above-developed renormalization prescription. Instead of calculating Eq. (2.6)

directly, we first evaluate the derivative of the effective potential, i.e.,^{35,36}

$$\frac{\partial V}{\partial \sigma} = i g_0 \text{tr} \int \frac{d^4 k}{(2\pi)^4} \frac{1}{g_0 \sigma - \not{k}} + m_0^2 \sigma, \quad (2.24)$$

where m_0^2 has already been fixed by Eq. (2.11). Calculating the integral which corresponds to the tadpole diagram and making use of the renormalization prescription in order to absorb the ϵ^{-1} part, we get the expression

$$\begin{aligned} \frac{\partial V}{\partial \sigma} = & -2M_0^2 \left(1 + \frac{5g^2}{24\pi^2}\right) \sigma + 2g^2 \left(1 + \frac{5g^2}{24\pi^2}\right) \sigma^3 \\ & - \frac{g^4}{4\pi^2} \sigma^3 \ln(g^2 \sigma^2 / M_0^2), \end{aligned} \quad (2.25)$$

where we have omitted R of σ_R and hereafter use this notation. Then, integration over the σ field leads us to the effective potential

$$\begin{aligned} V(\sigma) = & V_0 - M_0^2 \left(1 + \frac{5g^2}{24\pi^2}\right) \sigma^2 + \frac{1}{2} g^2 \left(1 + \frac{13g^2}{48\pi^2}\right) \sigma^4 \\ & - \frac{g^4}{16\pi^2} \sigma^4 \ln(g^2 \sigma^2 / M_0^2), \end{aligned} \quad (2.26)$$

where V_0 is a constant of integration. The effective potential $V_{\text{eff}}(\sigma) = V(\sigma) - V_0$ is plotted in Fig. 1. Here we use units in which $M_0 = 1$. As expected from the first, the origin of σ ($\sigma = 0$) is not a minimum of the effective potential, because Eq. (2.25) shows

$$\left. \frac{\partial V}{\partial \sigma} \right|_{\sigma=0} = 0, \quad (2.27)$$

$$\left. \frac{\partial^2 V}{\partial \sigma^2} \right|_{\sigma=0} = -2M_0^2 \left(1 + \frac{5g^2}{24\pi^2}\right) < 0, \quad (2.28)$$

so it corresponds to an unstable vacuum. The true minimum of the effective potential appears at $\sigma = \sigma_0$; indeed we can show

$$\left. \frac{\partial V}{\partial \sigma} \right|_{\sigma=\sigma_0} = 0, \quad (2.29)$$

$$\left. \frac{\partial^2 V}{\partial \sigma^2} \right|_{\sigma=\sigma_0} = \Delta^{-1}(k^2) \Big|_{\hbar\mu=0} = M_R^2 > 0. \quad (2.30)$$

This triggers off the violation of the chiral symmetry.

One more remarkable point about the effective potential comes from the behavior of large values of σ . In such a region, the fourth term with negative sign is dominant in Eq. (2.26), that is, as σ increases from 0 to ∞ , the effective potential decreases once, then reaches a minimum at $\sigma = \sigma_0$, next increases to attain a maximum at $\sigma \simeq \sigma_0 \exp(4\pi^2/g^2)$ for the small-coupling limit, and finally decreases again to $-\infty$. This implies that $\sigma = \sigma_0$ is not an absolute minimum, but a local

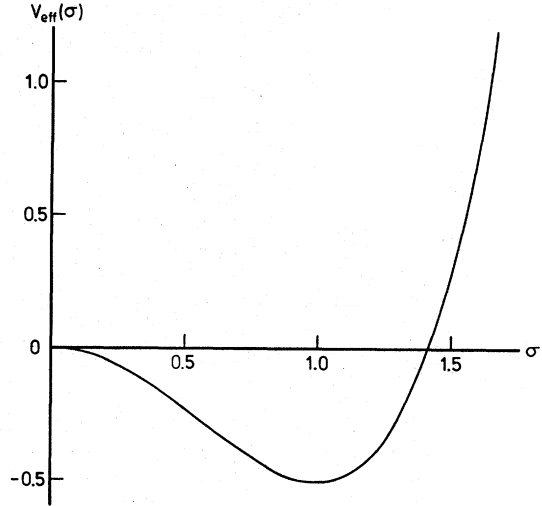


FIG. 1. Effective potential at $T=0$ and $\mu=0$.

stable vacuum, and the theory becomes unstable. If we work with perturbation about this vacuum, we would encounter a tachyon with a large negative mass squared. Indeed, we can show that besides the bound-state pole $k^2 = 4M_0^2$, the σ propagator has a tachyon pole $k^2 = -M_0^2 \exp(8\pi^2/g^2)$ for the small-coupling limit. This pole is well known as the *Landau ghost*,^{31,37,38} and is always accompanied by four-dimensional theory containing fermion-loop diagrams at large spacelike region. However, for the small coupling constant that is assumed in this theory, the ghost appears at a huge value of spacelike momentum, so it has no real significance in practice and the minimum at $\sigma = \sigma_0$ can be seen as a stable vacuum.

Finally we give N -point σ vertices $\Gamma^{(N)}$ ($N \geq 3$),

$$\Gamma^{(3)} = 12gM_0, \quad (2.31)$$

$$\Gamma^{(4)} = 12g^2 - \frac{3}{\pi^2} g^4, \quad (2.32)$$

$$\Gamma^{(N)} = \frac{3}{\pi^2} (-1)^N \frac{g^N}{M_0^{N-4}} \quad (N \geq 5), \quad (2.33)$$

which are given by differential coefficients of the effective potential at $\sigma = \sigma_0$.

III. GENERAL FORMULATION

In this section we study an effect of temperature T and fermion-number density n on the system which has been defined in the absence of both influences in the previous section. As will be shown later, fermion-number density relates directly to a chemical potential μ , so hereafter we often use μ instead of n . The symmetry-broken system, dependent on temperature and fermion-number den-

sity, can be described through the thermodynamic ensemble of the classical field σ ,

$$\sigma_0(T, \mu) \equiv \text{tr}(\rho\sigma) \quad (3.1)$$

with a weight function

$$\rho = \frac{e^{-(H-\mu N)/T}}{\text{tr} e^{-(H-\mu N)/T}}, \quad (3.2)$$

where H is the total Hamiltonian derived from the Lagrangian (2.1) and N represents a fermion-number operator defined in an antisymmetrized form

$$N = \frac{1}{2} \int d^3x [\bar{\psi}, \gamma_0 \psi]. \quad (3.3)$$

Because of the discussion in the previous section, the existence of a nonzero $\sigma_0(T, \mu)$ value in equilibrium generates a fermion mass as a function of T and μ ,

$$M(T, \mu) = g_0 \sigma_0(T, \mu), \quad (3.4)$$

which violates the chiral symmetry of the system, and the effective potential should satisfy the conditions

$$\left. \frac{\partial V}{\partial \sigma} \right|_{\sigma = \sigma_0(T, \mu)} = 0, \quad (3.5)$$

$$\left. \frac{\partial^2 V}{\partial \sigma^2} \right|_{\sigma = \sigma_0(T, \mu)} \geq 0. \quad (3.6)$$

All calculations in finite-temperature and finite-density theory can be performed, as usual, with the replacement of the usual Feynman propagator by the finite-temperature and finite-density Green's function. Thus, Eq. (3.5) gives an expression

$$m_0^2 \sigma_0(T, \mu) = g_0 T \sum_{N=-\infty}^{\infty} \text{tr} \int \frac{d^3\vec{k}}{(2\pi)^3} S_F^{(\beta)}(i\omega_N + \mu, \vec{k}), \quad (3.7)$$

which has the same role as Eq. (2.9). The $S_F^{(\beta)}(i\omega_N + \mu, \vec{k})$ is the finite-temperature and finite-density Green's function for fermions with mass $M(T, \mu)$ and an energy variable k_0 taking $i\omega_N + \mu$, where

$$\omega_N = (2N+1)\pi T, \quad N = 0, \pm 1, \pm 2, \dots \quad (3.8)$$

The summation $\sum_{N=-\infty}^{\infty}$ can be done with a conversion to a contour integral,⁵ and we get, with an energy $E = [\vec{k}^2 + M^2(T, \mu)]^{1/2}$,

$$m_0^2 \sigma_0(T, \mu) = -ig_0 \text{tr} \int \frac{d^4k}{(2\pi)^4} \frac{1}{M(T, \mu) - \not{k}} - \frac{g_0}{4\pi^3} M(T, \mu) \int \frac{d^3\vec{k}}{E} \left(\frac{1}{e^{(E-\mu)/T} + 1} + \frac{1}{e^{(E+\mu)/T} + 1} \right) \Big|_{E=[\vec{k}^2 + M^2(T, \mu)]^{1/2}}. \quad (3.9)$$

Because integrals over \vec{k} in the second term of Eq. (3.9) are convergent and an ultraviolet singularity appears only in the first term, we can introduce the same renormalization prescription as in Sec. II. Together with the value of m_0 fixed in Eq. (2.11) and with the use of the renormalization prescription, Eq. (3.9) turns out to be, besides a trivial solution $M(T, \mu) = 0$,

$$M^2(T, \mu) = M_0^2 - \frac{G^2}{8\pi^2} \int \frac{d^3\vec{k}}{E} \left(\frac{1}{e^{(E-\mu)/T} + 1} + \frac{1}{e^{(E+\mu)/T} + 1} \right) \Big|_{E=[\vec{k}^2 + M^2(T, \mu)]^{1/2}} \quad (3.10)$$

with

$$G^2 = \frac{24g^2}{24\pi^2 + 5g^2}, \quad (3.11)$$

where M_0 stands for the fermion mass generated in the $T = \mu = 0$ system. We may call Eq. (3.10) the self-consistency equation, because it plays the same role as the gap equation in the theory of type-II superconductivity.³⁹

As mentioned before, the chemical potential μ relates to the fermion-number density n . The n can be defined as a thermodynamical average of N , and with the use of the finite-temperature and finite-density Green's function $S_F^{(\beta)}$ it has an expression

$$\begin{aligned} n &= \text{tr}(\rho N) \\ &= -T \sum_{N=-\infty}^{\infty} \int \frac{d^3\vec{k}}{(2\pi)^3} \text{tr} \gamma_0 S_F^{(\beta)}(i\omega_N + \mu, \vec{k}) \\ &= 2 \int \frac{d^3\vec{k}}{(2\pi)^3} \left(\frac{1}{e^{(E-\mu)/T} + 1} - \frac{1}{e^{(E+\mu)/T} + 1} \right) \Big|_{E=[\vec{k}^2 + M^2(T, \mu)]^{1/2}}. \end{aligned} \quad (3.12)$$

The first and second terms in the last equality in the above equation correspond to the number density of

fermion and antifermion, respectively. The factor 2 in it comes from the spin degrees of freedom. Using Eq. (3.12), we can determine fermion-number density n by temperature T and chemical potential μ , also inversely μ by T and n . In a thermodynamical theory, it is conventional to specify the generated fermion mass M in terms of T and n , so we use the notation $M(T, n)$ instead of $M(T, \mu)$.

The calculation of the effective potential at finite temperature and finite density can also be done in the same manner as in Sec. II. Thus, we get

$$\begin{aligned} \frac{\partial V}{\partial \sigma} = & \left(\frac{\partial V}{\partial \sigma} \right)_0 - \frac{g^2}{4\pi^3} \int \frac{d^3\vec{k}}{E} \left(\frac{1}{e^{(E-\mu)/T} + 1} + \frac{1}{e^{(E+\mu)/T} + 1} \right) \sigma \Big|_{E=[\vec{k}^2 + M^2(T, \mu)]^{1/2}} \\ & + \frac{g^2}{4\pi^3} \int \frac{d^3\vec{k}}{E} \left(\frac{1}{e^{(E-\mu)/T} + 1} + \frac{1}{e^{(E+\mu)/T} + 1} \right) \sigma \Big|_{E=[\vec{k}^2 + g^2 \sigma^2]^{1/2}}, \end{aligned} \quad (3.13)$$

where $(\partial V/\partial \sigma)_0$ is the same expression as Eq. (2.25) with a replacement of M_0 by $M(T, \mu)$. We are going to investigate a behavior of the effective potential with the self-consistency equation (3.10) which determines the generated fermion mass and with Eq. (3.12), which give a mutual relation between n , μ , and T . In the following sections, we consider three cases to clear our discussion: $T \neq 0$, $\mu = 0$, then $T = 0$, $\mu \neq 0$, and finally $T \neq 0$, $\mu \neq 0$.

IV. $T \neq 0$ AND $\mu = 0$

In this case the system contains equal numbers of fermions and antifermions, so that total fermion-number density n vanishes, that can be shown by Eq. (3.12) with $\mu = 0$. Thus, the self-consistency equation (3.10) which determines the generated fermion mass becomes

$$M^2(T) = M_0^2 - \frac{G^2}{4\pi} \int \frac{d^3\vec{k}}{E} \left(\frac{1}{e^{(E/T)} + 1} \right) \Big|_{E=[\vec{k}^2 + M^2(T)]^{1/2}} \quad (4.1)$$

and is manipulated as follows:

$$M^2(T) = M_0^2 - G^2 M^2(T) \int_1^\infty dx (x^2 - 1)^{1/2} \frac{1}{e^{xM(T)/T} + 1} \quad (4.2)$$

$$= M_0^2 - G^2 M(T) T \sum_{n=1}^\infty \frac{(-1)^n}{n} K_1 \left(n \frac{M(T)}{T} \right), \quad (4.3)$$

where, and hereafter, $K_n(x)$ denotes the modified Bessel function of the second kind. Since the integral on the right-hand side of Eq. (4.1) or (4.2) is positive definite, then for any T the mass $M(T)$ generated at a finite temperature is less than M_0 at zero temperature. If there exists a temperature at which the generated fermion mass vanishes, the broken chiral symmetry is restored and we can define the temperature as a critical one, T_c . The critical temperature can be determined by Eq. (4.1) with $M(T_c) = 0$,

$$0 = M_0^2 - G^2 \int_0^\infty dE \frac{E}{e^{E/T_c} + 1} \quad (4.4)$$

and it turns out to be

$$T_c^2 = \frac{12}{\pi^2} \frac{M_0^2}{G^2}. \quad (4.5)$$

Between $T = 0$ and $T = T_c$, it holds that $M_0 \geq M(T) \geq 0$. With the use of an asymptotic expansion of the K_1 , we can give the behavior of Eq. (4.3) for low temperature $T \sim 0$, where $M(T)/T \gg 1$,

$$M^2(T) = M_0^2 - \sqrt{\pi/2} G^2 T^2 \sqrt{M_0/T} \left(1 + \frac{3}{8} \frac{T}{M_0} \right) e^{-M_0/T}. \quad (4.6)$$

Near the critical temperature $T \sim T_c$, where $M(T)/T \ll 1$, we can show that the generated fermion mass decreases to zero such that

$$M^2(T) = M_0^2 \left(1 - \frac{T^2}{T_c^2} \right). \quad (4.7)$$

Above the critical temperature Eq. (4.1) has no real solutions and Eq. (3.5) or (3.9) has only a trivial solution, so $\sigma_0(T) = 0$, then $M(T) = 0$. We can say that the chiral symmetry of the theory becomes restored for $T \geq T_c$. With the numerical calculation of Eqs. (4.3), (4.5), (4.6), and (4.7), we plot in Fig. 2 the generated fermion mass $M(T)$ as a function of T for the full range. This is a well-known behavior for several theories with a restoration of broken symmetry at finite temperature, and also shows similar behavior to the gap energy as a function of temperature⁴⁰ in the theory of superconductivity, for Eq. (4.1) plays the same role as the gap equation in that theory.

Now with the $M(T)$ fixed as a solution of Eq. (4.1), we are going to calculate the effective potential in the case $T \neq 0$, $\mu = 0$. Using the integral representation of the modified Bessel function for Eq. (3.13) with $\mu = 0$, we get

$$\begin{aligned} \frac{\partial V}{\partial \sigma} = & \left(\frac{\partial V}{\partial \sigma} \right)_0 - \frac{2}{\pi^2} g^2 T M(T) \sum_{n=1}^\infty \frac{(-1)^{n+1}}{n} K_1 \left(n \frac{M(T)}{T} \right) \sigma \\ & + \frac{2}{\pi^2} g^3 T \sigma^2 \sum_{n=1}^\infty \frac{(-1)^{n+1}}{n} K_1 \left(n \frac{g\sigma}{T} \right) \end{aligned} \quad (4.8)$$

and an integration over the σ variable gives the effective potential

$$\begin{aligned}
 V(\sigma) = & V_0 - M^2(T) \left(1 + \frac{5g^2}{48\pi^2}\right) \sigma^2 \\
 & + \frac{1}{2} g^2 \left(1 + \frac{13g^2}{48\pi^2}\right) \sigma^4 - \frac{g^4}{16\pi^2} \sigma^4 \ln [g^2 \sigma^2 / M^2(T)] \\
 & - \frac{g^2}{\pi^2} T M(T) \sigma^2 \sum_{n=1}^{\infty} \frac{(-1)^{n+1}}{n} K_1 \left(n \frac{M(T)}{T}\right) \\
 & - \frac{2g^2}{\pi^2} T^2 \sigma^2 \sum_{n=1}^{\infty} \frac{(-1)^{n+1}}{n^2} K_2 \left(n \frac{g\sigma}{T}\right), \quad (4.9)
 \end{aligned}$$

where V_0 is a constant of integration and we have made use of the relation

$$\frac{d}{z dz} [z^2 K_2(z)] = -z K_1(z). \quad (4.10)$$

By this effective potential we can investigate the model in several aspects. First, we define the inverse propagator of the σ field at zero four-momentum as

$$\Delta^{-1}(0) \Big|_{\sigma=\sigma_0(T)} = \frac{\partial^2 V}{\partial \sigma^2} \Big|_{\sigma=\sigma_0(T)}. \quad (4.11)$$

The right-hand side of the above equation is easily evaluated by Eq. (4.8) and turns out to be

$$\begin{aligned}
 \Delta^{-1}(0) \Big|_{\sigma=\sigma_0(T)} = & 4M^2(T) \left[\left(1 + \frac{g^2}{12\pi^2}\right) \right. \\
 & \left. - \frac{g^2}{2\pi^2} \sum_{n=1}^{\infty} (-1)^{n+1} K_0 \left(n \frac{M(T)}{T}\right) \right] \quad (4.12)
 \end{aligned}$$

with the help of the formula

$$z \frac{d}{dz} K_1(z) = -K_1(z) - z K_0(z). \quad (4.13)$$

It is seen from Eq. (4.12) that

$$\Delta^{-1}(0) \Big|_{\sigma=\sigma_0(T_c)} = 0 \quad (4.14)$$

because the generated fermion mass vanishes at $T = T_c$, $M(T_c) = 0$. Then the σ -propagator diverges at $T = T_c$ and it means that the model triggers off the second-order phase transition at this critical temperature. Equation (4.12), however, has one more zero point at $T = T_c^*$, satisfying the equation

$$1 + \frac{g^2}{12\pi^2} - \frac{g^2}{2\pi^2} \sum_{n=1}^{\infty} (-1)^{n+1} K_0 \left(n \frac{M(T_c^*)}{T_c^*}\right) = 0 \quad (4.15)$$

with nonzero finite mass $M(T_c^*)$, from which it is seen that T_c^* is below T_c . The amount of $M(T_c^*)$ can be estimated with the assumption $M(T_c^*)/T_c^* \ll 1$ as

$$M(T_c^*) \simeq T_c^* e^{-4\pi^2/g^2} \neq 0 \quad (4.16)$$

for a small coupling constant g . The curvature of the effective potential, $\partial^2 V / \partial \sigma^2 \Big|_{\sigma=\sigma_0(T)}$, changes its sign at "true" critical temperature T_c^* before T_c given by Eq. (4.5), and the squared renormalized mass of σ which is given by $\Delta^{-1}(0) \Big|_{\sigma=\sigma_0(T)}$ takes a negative value for $T_c^* < T \leq T_c$, i. e.,

$$\Delta^{-1}(0) \Big|_{\sigma=\sigma_0(T)} = M_R^2(T) \leq 0, \quad \text{for } T_c^* < T \leq T_c. \quad (4.17)$$

This implies that in the neighborhood of the phase-transition temperature for $T_c^* < T < T_c$, a tachyon would appear. Then the theory becomes unstable and could not be developed within approximation near such a region of T . But, for weak coupling, the right-hand side of Eq. (4.16) becomes tiny, and practically we may regard that

$$M(T_c^*) \simeq M(T_c) = 0. \quad (4.18)$$

Thus we can predict from a practical standpoint that the model has a second-order phase-transition temperature T_c ($\simeq T_c^*$). We illustrate $M_R^2(T) [= \Delta^{-1}(0) \Big|_{\sigma=\sigma_0(T)}]$ determined by Eq. (4.12) with fixed value of the generated fermion mass $M(T)$ as a function of T in Fig. 3.

Next, it is of interest to calculate the effective potential at $\sigma = 0$, because it relates to the total energy density of the massless fermion. By Eq.

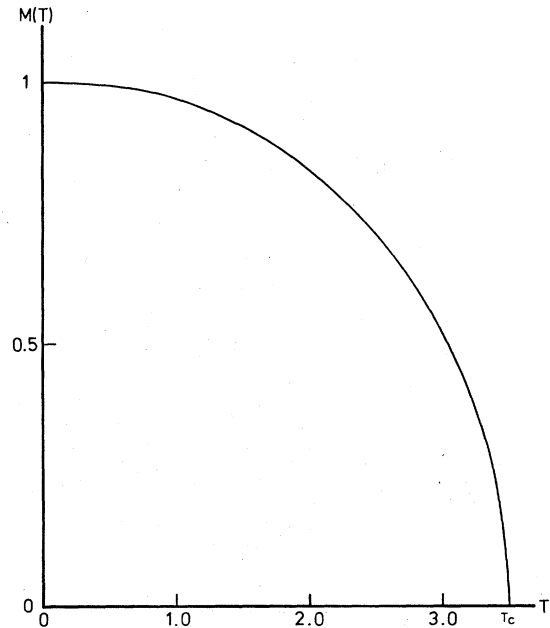


FIG. 2. Generated fermion mass as a function of temperature. T_c is the critical temperature.

(4.9), we find that

$$V(\sigma=0) = V_0 - \frac{2}{3\pi^2} \int_0^\infty dE \frac{E^3}{e^{E/T} + 1}, \quad (4.19)$$

and the total energy density E turns out to be

$$\begin{aligned} E &= -3V(\sigma=0) \\ &= E_0 + \frac{7}{60} \pi^2 T^4, \end{aligned} \quad (4.20)$$

where we identify $E_0 = -3V_0$. This is the famous "Stephan-Boltzman law"^{8,41} for a massless fermion-antifermion gas in thermal equilibrium and relates to the well-known blackbody radiation as

$$\begin{aligned} E &= E(\text{fermion}) + E(\text{antifermion}) \\ &= \frac{7}{4} \times (\text{energy of blackbody radiation}). \end{aligned} \quad (4.21)$$

Making use of the numerical solution of $M(T)$, we plot the shifted effective potential V_{eff} ,

$$V_{\text{eff}}(\sigma) = V(\sigma) - V(\sigma=0), \quad (4.22)$$

as a function of σ in Fig. 4. We can see from this figure that as temperature increases $\sigma = \sigma_0(T)$, the minimum of the effective potential, decreases, the depth of the effective potential becomes shallow, and thus the broken symmetry of the system is going to be lost.

Finally, we study the behavior of three- and four-point σ vertices when the temperature increases. Differentiating Eq. (4.8) successively

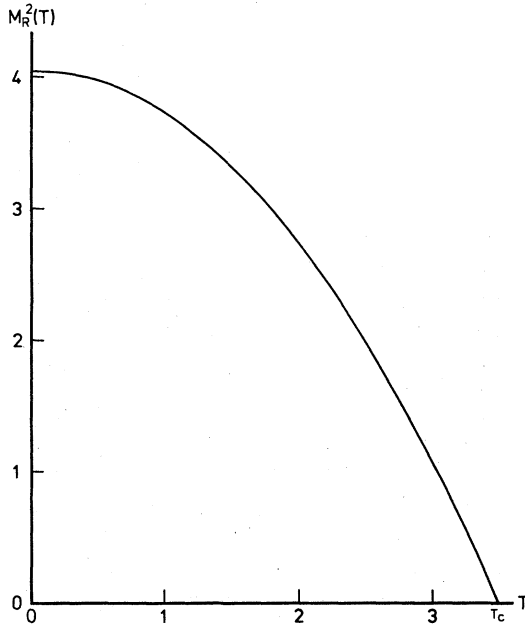


FIG. 3. Renormalized σ mass as a function of temperature.

and setting $\sigma = \sigma_0(T)$, we obtain $\Gamma^{(3)}(T)$ and $\Gamma^{(4)}(T)$ as follows:

$$\begin{aligned} \Gamma^{(3)}(T) &= 12gM(T) - \frac{6}{\pi^2} g^3 M(T) \sum_{n=1}^{\infty} (-1)^{n+1} K_0\left(n \frac{M(T)}{T}\right) \\ &\quad + \frac{2}{\pi^2} g^3 \frac{M^2(T)}{T} \sum_{n=1}^{\infty} (-1)^{n+1} n K_1\left(n \frac{M(T)}{T}\right) \end{aligned} \quad (4.23)$$

and

$$\begin{aligned} \Gamma^{(4)}(T) &= 12g^2 - \frac{3}{\pi^2} g^4 - \frac{6}{\pi^2} g^4 \sum_{n=1}^{\infty} (-1)^{n+1} K_0\left(n \frac{M(T)}{T}\right) \\ &\quad + \frac{8}{\pi^2} g^4 \frac{M(T)}{T} \sum_{n=1}^{\infty} (-1)^{n+1} n K_1\left(n \frac{M(T)}{T}\right) \\ &\quad - \frac{2}{\pi^2} g^4 \left(\frac{M(T)}{T}\right)^2 \sum_{n=1}^{\infty} (-1)^{n+1} n^2 K_0\left(n \frac{M(T)}{T}\right). \end{aligned} \quad (4.24)$$

These functions are shown in Figs. 5 and 6. When the temperature approaches the critical one T_c , the three- σ vertex as well as the renormalized σ mass goes to zero, which corresponds to the fact that the broken symmetry is restored, because the symmetry violation is due to an existence of these terms. However, near T_c , the four- σ vertex behaves like $\ln M(T)/T$ and then the model exhibits an infrared singularity at $T = T_c$. This implies that the perturbation expansion near the critical temperature goes meaningless even if we take a small coupling constant. The appearance of the infrared sing-

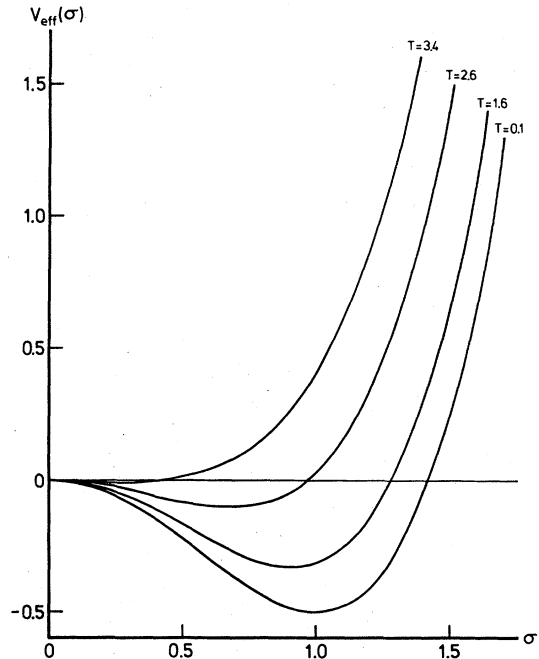
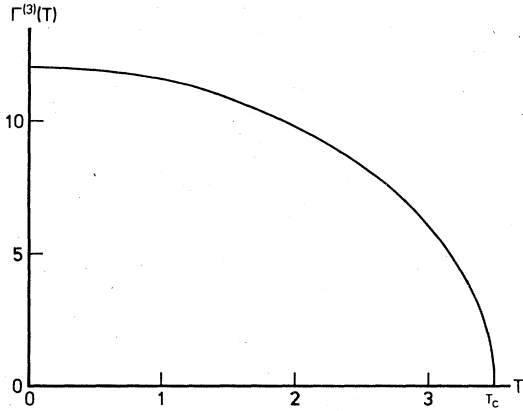


FIG. 4. Effective potential as a function of σ with several different values of temperature.

FIG. 5. Three- σ vertex as a function of temperature.

ularity is like the one in the work of Coleman and Weinberg,⁴² where infrared singularity locates at the origin of the classical field $M=0$ in their φ^4 effective potential. In our work $\sigma_0(T)$, which is dynamically generated and plays the same role as M in their work, necessarily goes to zero near the critical temperature and we cannot avoid an infrared singularity, that is the general feature of the model with the dynamically broken symmetry.

V. $T=0$ AND $\mu \neq 0$

When a system is at absolute zero temperature, it is completely degenerate and here the role of the antifermion vanishes. The fermion-number density is given by

$$n = 2 \int \frac{d^3\vec{k}}{(2\pi)^3} \theta(\mu - E) \Big|_{E=|\vec{k}+M^2(\mu)|^{1/2}} \\ = \frac{1}{3\pi^3} P_F^3, \quad (5.1)$$

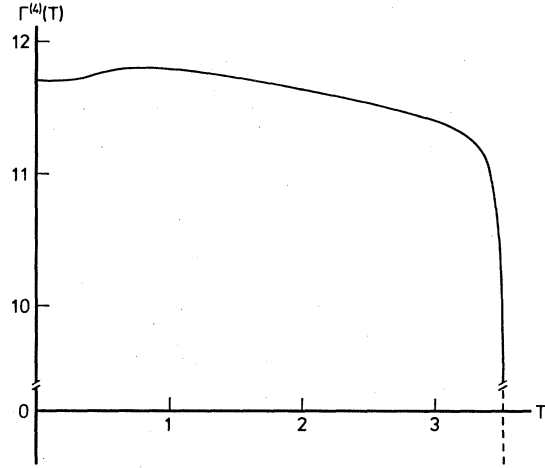
where $M(\mu)$ denotes the generated fermion mass which is of course a function of only μ or n , and P_F is the Fermi momentum

$$P_F^2 + M^2(\mu) = \mu^2. \quad (5.2)$$

The step function in Eq. (5.1) comes from the first term of the integrand in Eq. (3.12) and the second term there which corresponds to the number density of the antifermions does not contribute at $T \rightarrow 0$. With the above characteristic that antifermions have no contribution to the system in mind, we develop discussion in the same manner as in the previous section.

The self-consistency equation (3.10) turns out to be

$$M^2(\mu) = M_0^2 - \frac{G^2}{8\pi^2} \int \frac{d^3\vec{k}}{E} \theta(\mu - E) \Big|_{E=|\vec{k}^2+M^2(\mu)|^{1/2}}, \quad (5.3)$$

FIG. 6. Four- σ vertex as a function of temperature.

where we have already dropped the trivial solution $M(\mu)=0$. Equation (5.3) can be easily integrated to

$$M^2(\mu) = M_0^2 - \frac{G^2}{4} \left\{ \mu [\mu^2 - M^2(\mu)]^{1/2} - M^2(\mu) \ln \left[\frac{\mu + [\mu^2 - M^2(\mu)]^{1/2}}{M(\mu)} \right] \right\}. \quad (5.4)$$

A critical chemical potential μ_c as well as the critical temperature in Sec. IV can be defined by the condition

$$M(\mu_c) = 0, \quad (5.5)$$

and with Eq. (5.4) at $\mu = \mu_c$ we get

$$\mu_c = \frac{2}{G} M_0. \quad (5.6)$$

We cannot solve Eq. (5.4) analytically with respect to $M(\mu)$, but near the critical chemical potential, where we can assume $M(\mu)/\mu \ll 1$, the behavior of the generated fermion mass can be approximately shown to be like

$$M^2(\mu) \simeq M_0^2 \left(1 - \frac{\mu^2}{\mu_c^2} \right). \quad (5.7)$$

It is noted that the above equation has the same form as Eq. (4.7) in the $T \neq 0$ system except for the difference of parameters μ and T . We are able to draw the behavior of $M(\mu)$ for the full μ range with numerical calculations and to show that the $M(\mu)$ behaves similarly to the $M(T)$ calculated in the previous section, but in such a system it is conventional to specify the physical quantities as a function of the fermion-number density n . The n and μ are directly related through Eqs. (5.1), (5.2), and (5.4), but unfortunately the explicit expression of this relation cannot be given because we do not know the an-

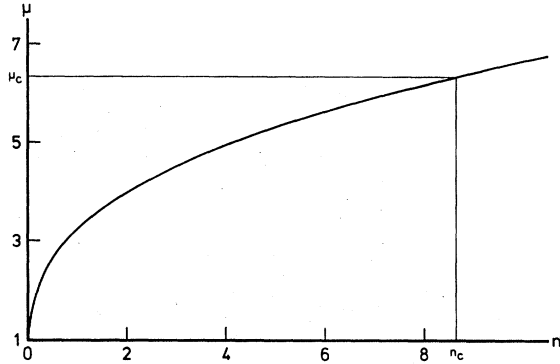


FIG. 7. Relation between number density and chemical potential. We use the unit $M_0=1$.

alytic solution of Eq. (5.4) with respect to $M(\mu)$. So, making use of Eqs. (5.1) and (5.2) and the numerical solution of Eq. (5.4), we exhibit the $n-\mu$ relation schematically in Fig. 7, where M_0 is taken as a unit of μ . The critical density n_c drawn in Fig. 5 is calculated exactly with the condition

$$M(n_c)=0, \tag{5.8}$$

and Eqs. (5.1), (5.2), and (5.6) give

$$n_c = \frac{8}{3\pi^2} \left(\frac{M_0}{\sqrt{G}} \right)^3. \tag{5.9}$$

Using the above numerical $\mu-n$ relation, we plot the behavior of the generated fermion mass M as a function of fermion-number density n in Fig. 8. Near the origin of n , $M(n)$ decreases

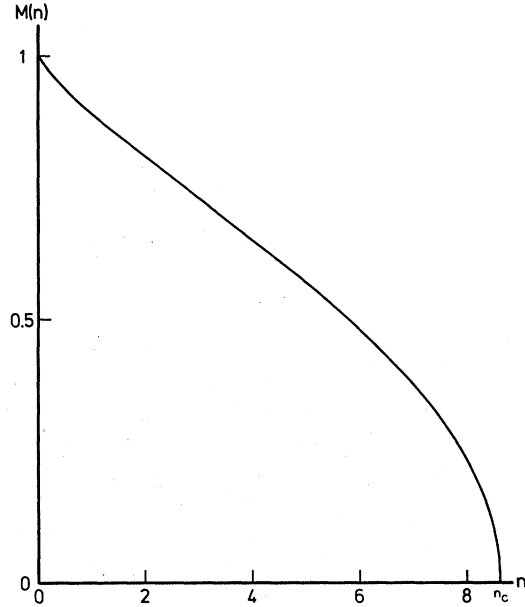


FIG. 8. Generated fermion mass as a function of number density at $T=0$. The n_c is the critical density.

more rapidly than the case of $M(T)$ for $T \approx 0$. By this figure it is noted that the dynamically violated chiral symmetry can be restored as fermion-number density increases.

The effective potential for this completely degenerate system is obtained through Eq. (3.13) with $T=0$ and an integration of such an equation over the classical σ field gives

$$\begin{aligned} V(\sigma) = & V_0 - M^2(\mu) \left(1 + \frac{5g^2}{24\pi^2} \right) \sigma^2 + \frac{1}{2} g^2 \left(1 + \frac{13g^2}{48\pi^2} \right) \sigma^4 - \frac{g^4}{16\pi^2} \sigma^4 \ln[g^2 \sigma^2 / M^2(\mu)] \\ & - \frac{g^2}{4\pi^2} \{ \mu [\mu^2 - M^2(\mu)]^{1/2} - M^2(\mu) \ln [(\mu + [\mu^2 - M^2(\mu)]^{1/2}) / M(\mu)] \} \sigma^2 \\ & + \frac{\mu}{24\pi^2} (5g^2 \sigma^2 - 2\mu^2) (\mu^2 - g^2 \sigma^2)^{1/2} - \frac{g^4}{8\pi^2} \sigma^4 \ln \{ [\mu + (\mu^2 - g^2 \sigma^2)^{1/2}] / (g\sigma) \}, \end{aligned} \tag{5.10}$$

where V_0 is a constant of integration which differs from one in the previous section. From Eq. (5.10) we find that

$$V(\sigma=0) = V_0 - \frac{1}{12\pi^2} \mu^4. \tag{5.11}$$

$V(\sigma=0)$ relates to the total energy density of the completely degenerate system of massless fermions⁴¹ for

$$\begin{aligned} E = & -3V(\sigma=0) \\ = & E_0 + 2 \int \frac{d^3 \vec{k}}{(2\pi)^3} |\vec{k}| \theta(\mu - |\vec{k}|) \\ = & E_0 + \frac{1}{4\pi^2} \mu^4. \end{aligned} \tag{5.12}$$

Shifting the origin of $V(\sigma)$, we plot

$$V_{\text{eff}}(\sigma) = V(\sigma) - V(\sigma=0) \quad (5.13)$$

for several values of n in Fig. 9, where we have used the numerical solution of $M(\mu)$. We observe from this figure that the symmetry under the effect only of number density behaves as one under the temperature effect, and that when the number density increases above the critical value, the broken symmetry begins to be lost.

The inverse σ propagator in this case is calculated in the manner worked previously and we get

$$\Delta^{-1}(0)|_{\sigma=\sigma_0} = 4M^2(\mu) \left[\left(1 + \frac{g^2}{12\pi^2} \right) - \frac{g^2}{4\pi^2} \ln \left\{ \frac{\mu + [\mu^2 - M^2(\mu)]^{1/2}}{M(\mu)} \right\} \right]. \quad (5.14)$$

Here the same phenomenon is seen as already observed in the finite-temperature system, that is, besides $M(\mu_c) = 0$, the σ propagator has one other pole at $n = n_c^*$ (or $\mu = \mu_c^*$) satisfying

$$\left(1 + \frac{g^2}{12\pi^2} \right) - \frac{g^2}{4\pi^2} \ln \left\{ \frac{\mu_c^* + [\mu_c^{*2} - M^2(\mu_c^*)]^{1/2}}{M(\mu_c^*)} \right\} = 0. \quad (5.15)$$

Just as in Sec. IV, we can see that

$$n_c^* < n_c \quad (\text{or } \mu_c^* < \mu_c), \quad (5.16)$$

and the generated fermion mass at $\mu = \mu_c^*$ is estimated for the weak-coupling limit,

$$M(\mu_c^*) \simeq \mu_c^* e^{-4\pi^2/g^2}. \quad (5.17)$$

So, in the neighborhood of the phase-transition density $n_c^* < n < n_c$ (or $\mu_c^* < \mu < \mu_c$), a curvature of

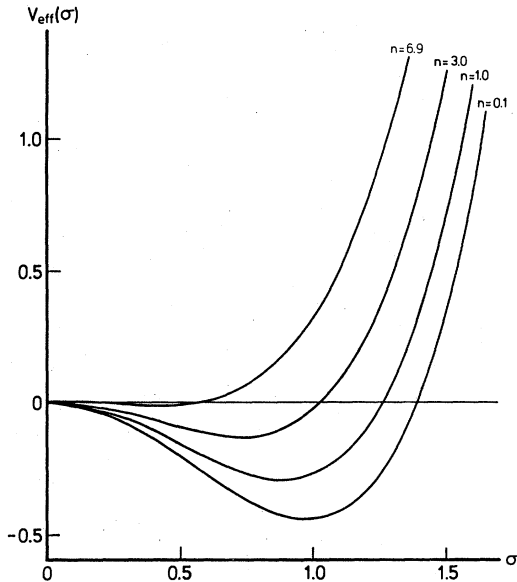


FIG. 9. Effective potential as a function of σ with several different values of number density at $T=0$.

$V(\sigma)$ becomes negative, i.e., the renormalized σ mass squared is negative:

$$M_R^2(n) = \Delta^{-1}(0)|_{\sigma=\sigma_0(n)} < 0, \quad (5.18)$$

and then approximation may be broken down because of the existence of tachyons. However, as discussed in Sec. IV, we can consider in a practical manner that at $n = n_c$ (or $\mu = \mu_c$), the generated fermion mass Eq. (5.17) is vanishing for the weak-coupling limit; then we may observe that the system has the second-order phase-transition density n_c above which the chiral symmetry is restored. In Fig. 10 we illustrate the renormalized σ mass as a function of n where we have used the numerical value of the generated fermion mass $M(\mu)$ satisfying Eq. (5.3) or (5.4).

The three- and four- σ vertices are computed by the third and fourth derivative of $V(\sigma)$ at

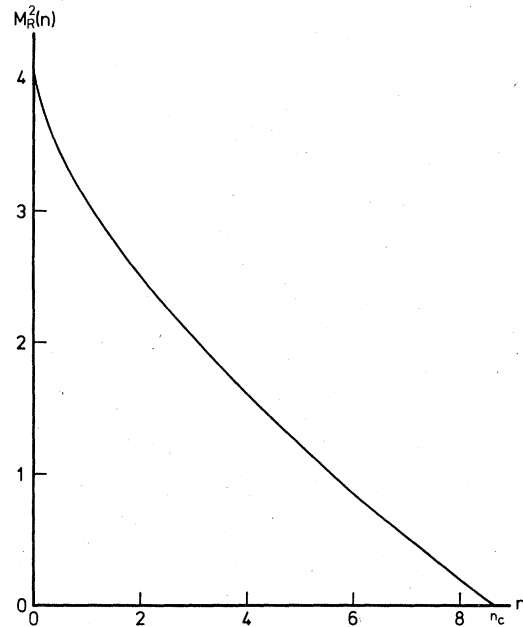


FIG. 10. Renormalized σ mass as a function of n .

$\sigma = \sigma_0$, respectively, and we write them as follows:

$$\Gamma^{(3)}(\mu) = 12gM(\mu) + \frac{\mu M(\mu)}{[\mu^2 - M^2(\mu)]^{1/2}} - \frac{3}{\pi^2} g^3 M(\mu) \ln\left\{\frac{\mu + [\mu^2 - M^2(\mu)]^{1/2}}{M(\mu)}\right\} \quad (5.19)$$

and

$$\Gamma^{(4)}(\mu) = 12g^2 - \frac{3}{\pi^2} g^4 + \frac{g^4}{\pi^2} \mu \left(\frac{1}{[\mu^2 - M^2(\mu)]^{1/2}} \right)^3 [4\mu^2 - 3M^2(\mu)] - \frac{3}{\pi^2} g^4 \ln\left\{\frac{\mu + [\mu^2 - M^2(\mu)]^{1/2}}{M(\mu)}\right\}. \quad (5.20)$$

Making use of the numerical solution of $M(\mu)$ of Eq. (5.3) or (5.4) and the relation between n and μ , we show the behavior of $\Gamma^{(3)}$ and $\Gamma^{(4)}$ as a function of n in Figs. 11 and 12, respectively. As expected, $\Gamma^{(3)}(n)$ vanishes with an increase of fermion-number density n and, together with the vanishing of $M_R^2(n)$ at $n = n_c$, the broken symmetry of the system is restored. But $\Gamma^{(4)}(n)$ exhibits the infrared divergence near the critical density. This is the same phenomenon commented on in Eq. (4.24) in the previous section.

When we describe the formalism in terms of the chemical potential of the fermion instead of the fermion-number density, we find that M_R^2 , $\Gamma^{(3)}$, and $\Gamma^{(4)}$ as functions of μ in the region $\mu > M_0$, have similar behavior to Figs. 3; 11, and 12, respectively. In $\mu < M_0$, these functions are constants and are given by ones in Sec. II where $T = 0$ and $\mu = 0$. We can show that M_R^2 changes con-

tinuously at $\mu = M_0$, while $\Gamma^{(3)}$ and $\Gamma^{(4)}$ change discontinuously. These correspond to the divergence at $n = 0$ as illustrated in Figs. 11 and 12. This is because at the absolute zero temperature, the system is completely degenerate, where the Fermi distribution function becomes singular, $\theta(\mu - M(\mu))$.

VI. $T \neq 0$ AND $\mu \neq 0$

This is the most general case where the system is specified by both temperature and number density (or chemical potential). We begin this program by solving the self-consistency equation (3.10) and give a phase diagram in which the generated fermion mass is plotted as a function of T and n . The phase boundary lines at $n = 0$ in the $M(T, n) - T$ plane and at $T = 0$ in the $M(T, n) - n$ plane have already been obtained in Figs. 2 and 8, respectively. The boundary line at $M(T, n) = 0$ in the $T - n$ plane is obtained by putting $M(T, n) = 0$ in Eqs. (3.10) and (3.12), and they are manipulated as

$$\int_0^\infty dx x \left(\frac{1}{e^{x-\mu/T} + 1} + \frac{1}{e^{x+\mu/T} + 1} \right) = \frac{2M_0^2}{G^2 T^2} \quad (6.1)$$

and

$$n = \frac{T^3}{\pi^2} \int_0^\infty dx x^2 \left(\frac{1}{e^{x-\mu/T} + 1} - \frac{1}{e^{x+\mu/T} + 1} \right). \quad (6.2)$$

These integrations are easily calculated to give

$$\mu^2 = \frac{\pi^2}{3} (T_c^2 - T^2) \quad (6.3)$$

and

$$n = \frac{\mu}{\pi^2} \left(\mu_c^2 - \frac{2}{3} \mu^2 \right), \quad (6.4)$$

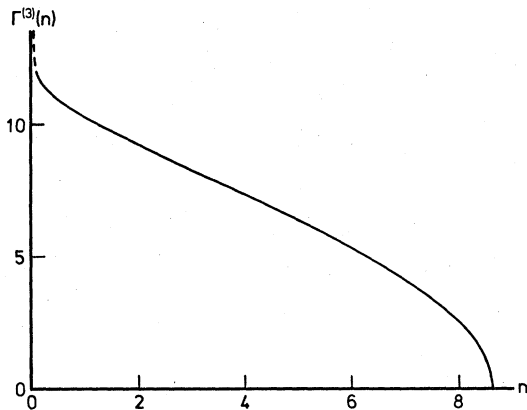


FIG. 11. Three- σ vertex as a function of n .

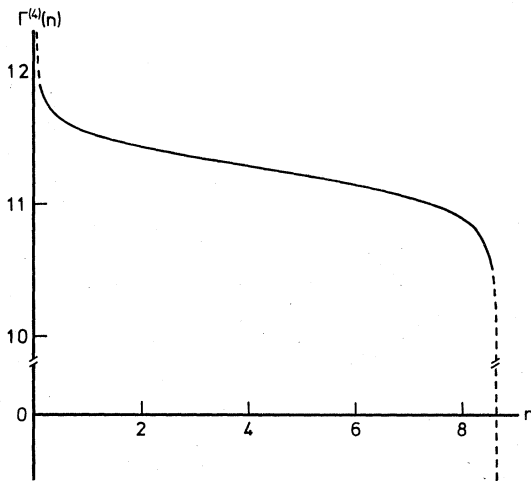


FIG. 12. Four- σ vertex as a function of n .

where T_c and μ_c are the already calculated critical temperature at $\mu=0$ and the critical chemical potential at $T=0$ in Eqs. (4.5) and (5.6), respectively. Eliminating μ from Eqs. (6.3) and (6.4), we get the $T-n$ relation in $M(T,n)=0$ and this is drawn in Fig. 13, which is the phase boundary line at $M(T,n)=0$ in $T-n$ plane. We find from Eqs. (6.3) and (6.4) or Fig. 13 that at sufficiently low temperature, the critical density increases together with temperature and when the temperature reaches $T_c/\sqrt{2}$, the critical density goes to a maximum, then turns into a decreasing function of temperature. On the other hand, the critical temperature is a decreasing function of number density. Especially, in a certain region of n , the diagram shows two critical temperatures and between them the symmetry-breaking phase occurs. The qualitative behavior of the phase diagram for the model $(\bar{\psi}\psi)^2$ is similar to one of the phase transition of an abnormal nuclear matter described by the σ model considered by Wakamatsu and Hayashi.⁴³ This may be a consequence of the *equivalence theorem*^{27, 30, 31} between the σ model and the $(\bar{\psi}\psi)^2$ theory with the appearance of collective excitations. The characteristic that the critical temperature is a two-valued function of n can be seen later in the behavior of the renormalized σ mass, three- σ , and four- σ vertices. The phase-boundary line at a nonzero value of $M(T,n)$ is obtained from Eqs. (3.10) and (3.12) numerically. With the boundary lines for several fixed values of $M(T,n)$ such that

$$0 \leq M(T,n) \leq M_0, \quad (6.5)$$

we have the generated mass of fermions as a function of T and n . This phase diagram is shown in Fig. 14. This figure shows the behavior of the generated fermion mass, which originates the violation of chiral symmetry, for the full T and n range.

Using the above-obtained numerical solution of $M(T,n)$, we can get a behavior of the effective potential for given T and n by numerical integration of Eq. (3.13). It seems needless to show this behavior because it resembles Figs. 4 and 9.

The renormalized σ mass, three- σ and four- σ vertices are all calculated from Eq. (3.13) as follows:

$$\begin{aligned} M_R^2(T, \mu) &= \left. \frac{\partial^2 V}{\partial \sigma^2} \right|_{\sigma=\sigma_0(T, \mu)} \\ &= 4M^2(T, \mu) \left[\left(1 + \frac{g^2}{12\pi^2} \right) - \frac{g^2}{4\pi^2} \int_1^\infty dx f(x) \right], \end{aligned} \quad (6.6)$$

$$\begin{aligned} \Gamma^{(3)}(T, \mu) &= \left. \frac{\partial^3 V}{\partial \sigma^3} \right|_{\sigma=\sigma_0(T, \mu)} \\ &= 12gM(T, \mu) + \frac{2g^3}{\pi^2} M(T, \mu) \int_1^\infty dx (x^2 - 2)f(x) \\ &\quad + \frac{g^3}{2\pi^2} \frac{M^2(T, \mu)}{T} \int_1^\infty dx x(x^2 - 2)g(x), \end{aligned} \quad (6.7)$$

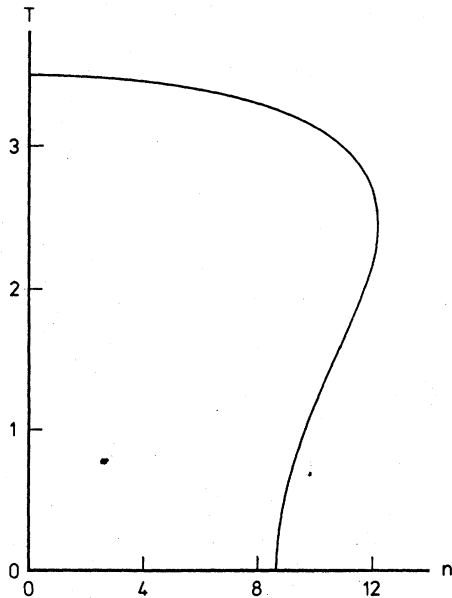


FIG. 13. Phase diagram in the $T-n$ plane.

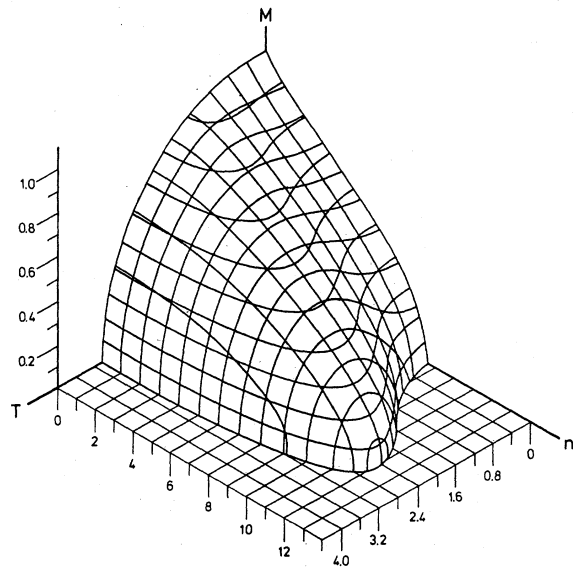


FIG. 14. Phase diagram.

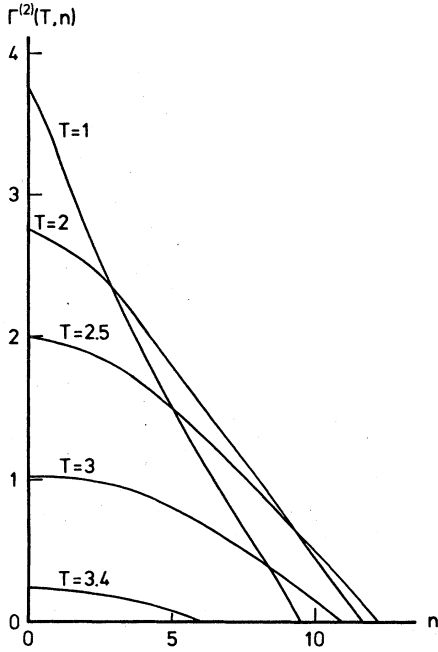


FIG. 15. Renormalized σ mass as a function of n with several different values of T .

$$\begin{aligned} \Gamma^{(4)}(T, \mu) &= \left. \frac{\partial^4 V}{\partial \sigma^4} \right|_{\sigma=\sigma_0(T, \mu)} \\ &= 12g^2 \left(1 - \frac{g^2}{4\pi^2} \right) + 2 \frac{g^4}{\pi^2} \int_1^\infty dx (x^2 - 2) f(x) \\ &\quad + 2 \frac{g^4}{\pi^2} \frac{M(T, \mu)}{T} \int_1^\infty dx x (x^2 - 2) g(x) \\ &\quad + \frac{g^4}{2\pi^2} \frac{M^2(T, \mu)}{T^2} \int_1^\infty dx x^2 (x^2 - 2) h(x), \end{aligned} \quad (6.8)$$

where

$$f(x) = \frac{1}{(x^2 - 1)^{1/2}} \left(\frac{1}{\exp(z_-)} + \frac{1}{\exp(z_+)} \right), \quad (6.9)$$

$$g(x) = \frac{1}{2(x^2 - 1)^{1/2}} [\operatorname{sech}^2(z_-/2) + \operatorname{sech}^2(z_+/2)], \quad (6.10)$$

$$\begin{aligned} h(x) &= \frac{1}{2(x^2 - 1)^{1/2}} \{ \tanh(z_-/2) [1 - \tanh^2(z_-/2)] \\ &\quad + \tanh(z_+/2) [1 - \tanh^2(z_+/2)] \}, \end{aligned} \quad (6.11)$$

$$z_\pm = \frac{xM(T, \mu) \pm \mu}{T}. \quad (6.12)$$

These expressions show that it is difficult or impossible for us to study the behavior of these quantities analytically as done in the previous two sections, so we only do a numerical search.

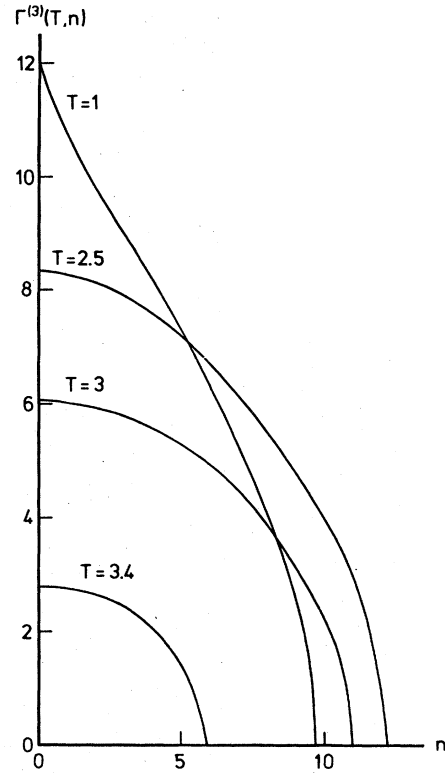


FIG. 16. Three- σ vertex as a function of n with several different values of T .

With numerical integration, we draw them as functions of density n for several fixed temperatures of T in Figs. 15–17, where we have made use of the numerical value of the generated fermion mass $M(T, \mu)$ satisfying Eq. (3.10) and the relation between n and μ . From these diagrams,

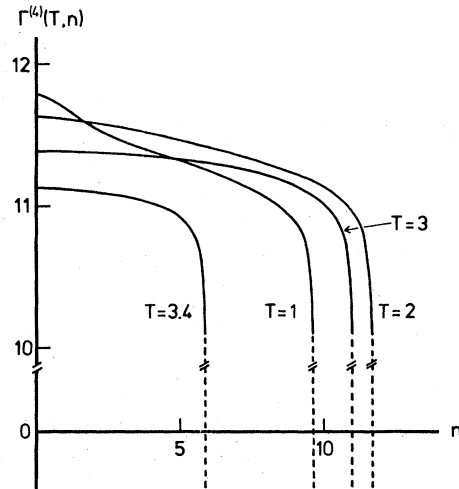


FIG. 17. Four- σ vertex as a function of n with several different values of T .

it is seen that the renormalized σ mass and three- σ vertex tend to vanish as the density increases and the four- σ vertex shows infrared divergence near the critical density as in the previous two sections. In these figures, the entanglement of curves for different fixed values of T implies that temperature is a two-valued function of density in the phase-boundary line diagram, which has already been noted.

ACKNOWLEDGMENTS

The authors would like to thank Dr. Shinji Nambu for valuable discussions. One of the authors (H.M.) is also indebted to Dr. Kenji Yoro for his help in the numerical calculations that are done in the Information Processing Research Center of Kwansai Gakuin University and the Data Processing Center of Kyoto University.

- ¹D. A. Kirzhnits and A. D. Linde, Phys. Lett. **42B**, 471 (1972).
²S. Weinberg, Phys. Rev. D **9**, 3357 (1974).
³L. Dolan and R. Jackiw, Phys. Rev. D **9**, 3320 (1974).
⁴C. W. Bernard, Phys. Rev. D **9**, 3312 (1974).
⁵M. B. Kislinger and P. D. Morley, Phys. Rev. D **13**, 2765 (1976); **13**, 2771 (1976).
⁶G. Baym and G. Grinstein, Phys. Rev. D **15**, 2897 (1977).
⁷L. R. Ram Mohan, Phys. Rev. D **14**, 2670 (1976); **15**, 3030 (1977).
⁸W. Dittrich, Phys. Rev. D **19**, 2385 (1979).
⁹R. N. Mohapatra and G. Senjanovic, Phys. Rev. D **20**, 3390 (1979).
¹⁰B. B. Deo and S. Kumar, Phys. Rev. D **12**, 3291 (1975).
¹¹P. D. Morley, Phys. Rev. D **17**, 598 (1978).
¹²L. Dolan, Phys. Rev. D **12**, 3098 (1975).
¹³T. D. Lee and G. C. Wick, Phys. Rev. D **9**, 2291 (1974).
¹⁴R. L. Bowers, A. M. Gleeson, and R. D. Pedigo, Phys. Rev. D **12**, 3043 (1975).
¹⁵R. L. Bowers, A. M. Gleeson, R. D. Pedigo, and J. W. Wheeler, Phys. Rev. D **15**, 2125 (1977).
¹⁶T. D. Lee and M. Margulies, Phys. Rev. D **11**, 1591 (1975).
¹⁷A. D. Linde, Phys. Rev. D **14**, 3345 (1976).
¹⁸D. J. Gross and A. Neveu, Phys. Rev. D **10**, 3235 (1974).
¹⁹L. Jacobs, Phys. Rev. D **10**, 3956 (1974).
²⁰B. J. Harrington and A. Yildiz, Phys. Rev. D **11**, 779 (1975); **11**, 1705 (1975).
²¹R. F. Dashen, S.-K. Ma, and R. Rajaraman, Phys. Rev. D **11**, 1499 (1975).
²²B. J. Harrington, S. Y. Park, and A. Yildiz, Phys. Rev. D **11**, 1472 (1975).
²³Y. Nambu and G. Jona-Lasinio, Phys. Rev. **122**, 345 (1961).
²⁴T. Eguchi and H. Sugawara, Phys. Rev. D **10**, 4257 (1974).
²⁵K. Kikkawa, Prog. Theor. Phys. **56**, 947 (1976).
²⁶T. Kugo, Prog. Theor. Phys. **55**, 2032 (1976).
²⁷S. Kawati and H. Miyata, Phys. Rev. D **21**, 1651 (1980).
²⁸F. Cooper, G. S. Guralnik, and S. H. Kasdan, Phys. Rev. D **14**, 1507 (1976).
²⁹N. Snyderman and G. S. Guralnik, in *Quark Confinement and Field Theory*, edited by D. Stump and D. Weingarten (Wiley, New York, 1977), p. 33.
³⁰T. Eguchi, Phys. Rev. D **14**, 2755 (1976); **17**, 611 (1978).
³¹K. Tamvakis and G. S. Guralnik, Phys. Rev. D **18**, 4551 (1978).
³²If, instead of the dimensional-regularization method, we introduce a cutoff parameter Λ , the renormalized coupling turns out to be the order of $1/\ln\Lambda^2$. In this case the model contains $\ln\Lambda^2$ implicitly in a final expression; for the Pauli-Villars regularization method, see Ref. 27.
³³G. 't Hooft and M. Veltman, Nucl. Phys. **B44**, 189 (1972).
³⁴J. M. Jauch and F. Rohrlich, *The Theory of Photons and Electrons* (Springer, New York, 1976), p. 460.
³⁵S. Y. Lee and A. M. Sciaccaluga, Nucl. Phys. **B96**, 435 (1975).
³⁶P. Rembiesa, Phys. Rev. D **18**, 4571 (1978).
³⁷J. Schwinger, *Particles, Sources, and Fields* (Addison-Wesley, Reading, Mass., 1973), Vol. II., p. 40.
³⁸E. M. Lifshitz and L. P. Pitaevskii, *Relativistic Quantum Field Theory, Part II* (Pergamon, Oxford, 1974); see also Ref. 31.
³⁹V. L. Ginzburg and L. D. Landau, Zh. Eksp. Teor. Fiz. **20**, 1064 (1950).
⁴⁰A. A. Abrikosov, L. P. Gorkov, and I. E. Szyaloshinski, *Quantum Field Theoretical Method in Statistical Physics* (Pergamon, Oxford, 1965).
⁴¹L. Landau and E. M. Lifshitz, *Statistical Physics* (Pergamon, London, 1959).
⁴²S. Coleman and E. Weinberg, Phys. Rev. D **7**, 1888 (1973); see also Ref. 2.
⁴³M. Wakamatsu and A. Hayashi, Prog. Theor. Phys. **63**, 1688 (1980).